Volume 16 Number 16 1988 Nucleic Acids Research

$Rh(DIP)_3^{3+}$: a shape-selective metal complex which targets cruciforms

Mindy R.Kirshenbaum, Roger Tribolet and Jacqueline K.Barton*

Department of Chemistry, Columbia University, New York, NY 10027, USA

Received April 28, 1988; Revised and Accepted July 20, 1988

ABSTRACT

The coordination complex tris(4,7-diphenylphenanthroline)rhodium(III), $Rh(DIP)_3^{3+}$, binds to and, upon photoactivation, cleaves both DNA strands near the base of a DNA cruciform. Sites of photoinduced double-stranded DNA cleavage by the rhodium complex map to regions containing cruciforms on closed circular pBR322, pColE1 and ϕX174 (replicative form) DNAs. Neither cleavage nor binding by the metal complex, assayed using S1 nuclease, is found on the linear plasmid which lacks the extruded cruciform. High resolution mapping experiments reveal that $Rh(DIP)_3^{3+}$ cleaves at a specific AT-rich site neighboring the stem of the minor cruciform on pBR322. The primary site of cleavage is found at position 3238 on the 3'-strand and 3250 on the 5'-strand and is remarkably specific. The pattern of cleavage, to one side only of the cruciform stem, indicates an asymmetry in the cruciform structure recognized by the complex. These results suggest that $Rh(DIP)_3^{3+}$ may provide a useful reagent to probe cruciform sites. In addition, the high degree of specificity found in targeting the cruciform structure with this simple metal complex underscores the utility of shape-selection for the recognition of specific sites on a DNA strand.

INTRODUCTION

There has been considerable interest in the design of molecules which interact at specific sites along the DNA strand, so as to develop site-selective probes for DNA structure, to develop chemical tools for biotechnology and to elucidate aspects of site-specific recognition of DNA. We have focused on the design of conformation-specific molecules (1). Coordinatively saturated metal complexes, lacking hydrogen bonding groups, have been prepared which are matched to DNA conformations based upon considerations of shape and symmetry. In particular, $Ru(TMP)_3^{2+}$ (TMP=Tris-3,4,7,8-tetramethylphenanthroline) binds preferentially to A-like conformations (2,3) and Λ–$Co(DIP)_3^{3+}$ (DIP=4,7-diphenyl-1,10-phenanthroline) recognizes conformationally distinct sites such as Z-DNA (4,5). Upon photoactivation, these complexes induce DNA strand scission at their site of binding (6).

Among the most dramatic variations in structure that may occur along the strand is the extrusion of inverted repeat sequences into cruciforms (7). Although the detailed structure of the cruciform has not yet been determined, in elegant studies (8) Lilley and co-workers have characterized the dynamics (9), sequence variation (10), and requirements (salt and superhelicity) (11) associated with cruciform formation. The single-stranded character of the intrastrand loops in cruciforms tends primarily to be the basis for their detection along the DNA strand using either

© IRL Press Limited, Oxford, England.

chemical probes, such as osmium tetroxide or bromacetaldehyde (12), or enzymatic probes such as S1 nuclease (13). Psoralen crosslinking of intrastrand hydrogen bonded segments also provides a useful chemical marker (14). Most novel, in terms of site-specific targeting, has been the enzymatic cleavage of the cruciform base by T4 endonuclease VII, developed based on the analogy between cruciform structures and Holliday structural intermediates in genetic recombination (15).

Here we report the unique targeting of a cruciform site with the metal complex tris(4,7-diphenylphenanthroline)rhodium(III), $Rh(DIP)_3^{3+}$. Upon photoactivation $Rh(DIP)_3^{3+}$ yields specific cleavage, which is primarily double-stranded, at the base of the DNA cruciform.

EXPERIMENTAL

Rhodium complexes and other chemicals

Tris(4,7-diphenyl-1,10-phenanthroline)rhodium(III) trichloride, $[Rh(DIP)_3]Cl_3$, was synthesized by the catalytic method of Gillard *et al.* (16). The crude product, a mixture of tris(diphenylphenanthroline) and bis(diphenylphenanthroline) species, is recrystallized from ethanol and saturated NaCl. A pink impurity, $[Fe(DIP)_3]Cl_2$, is removed by recrystallization from acetone to yield a beige solid. Elemental analysis found: C, 62.37; N 6.07; H 5.06%; Calculated for $C_{72}H_{72}N_6Cl_3O_{10}Rh$ ($[Rh(DIP)_3]Cl_3 \cdot 10H_20$) C 62.36; N, 6.06; H, 4.94%. Solution concentrations are determined spectrophotometrically using $\varepsilon_{296} = 1.16 \times 10^5\ M^{-1}\ cm^{-1}$. Rhodium trichloride trihydrate was obtained from Merck and the free DIP ligand was from Aldrich. Enantiomers of $[Rh(DIP)_3]Cl_3$ were separated by a modified method of Gillard *et al.* (17). The optical purity of both enantiomers was found to be greater than 90% by NMR experiments using a chiral shift reagent (18).

The DNAs pBR322 and ΦX174 (replicative form II) and all enzymes were obtained from Bethesda Research Laboratories. Plasmid pCol E1 was from Sigma. ^{32}P-labeled nucleotides were from NEN.

Photolysis

Irradiations for coarse mapping experiments were performed using either a 15 Watt Sylvania black light, with main output in the range 340-370 nm, or a 1000-W Hg/Xe lamp (Oriel Corporation of America) focused to 315 ± 6 nm. Irradiations for fine mapping experiments were performed using the 1000 W Hg/Xe lamp focused to 332 ± 6 nm.

Coarse mapping procedure

$[Rh(DIP)_3]Cl_3$ (10 μM) is added to plasmid DNA (100 μM nucleotide) in 50 mM Tris acetate buffer, pH 7.0, containing 18 mM sodium chloride NaCl. The 20 μL sample is subsequently irradiated for 10 min. using the Sylvania black light or for 20-60 sec using the 1000W Hg/Xe lamp and then ethanol precipitated. Under these conditions, photolysis yields partial to complete conversion to form II and form III DNA. After resuspension in the appropriate enzyme reaction buffer, restriction enzyme is added in excess to insure complete linearization. The DNA-enzyme mixture is then digested at 37 C for 1.5 h. For subsequent digestion with S1 nuclease, the pH of

the reaction buffer is then adjusted to 6.0, $ZnSO_4$ is added to a final concentration of 1 mM, 10-20 units S1 nuclease is added, and the sample is incubated for 20 min at 37 C. This reaction is quenched with the addition of bromphenol blue dye containing 50% sucrose, 0.5% bromphenol blue, 10 mM EDTA. Electrophoresis on 1% agarose gels (50 mM tris acetate, 18 mM NaCl, pH 7.0) resolves the specific fragments produced. Gels are stained with 1 μg/ml ethidium bromide for 0.5 h and then photographed with a Polaroid 600 camera equipped with red filter and 655 positive/negative film, with gels irradiated from below. For experiments with plasmid ColE1, and the replicated form of ΦX174, irradiation times were increased to 120 and 100 seconds, respectively. Densitometric scans are performed on photographic negatives using an LKB 2202 ultrascan laser densitometer coupled through a Nelson Interface to an IBM PC. The lengths of fragments are quantitated relative to markers of known molecular weight. Plasmid pBR322 sequences are numbered beginning at the EcoRI site as described by Sutcliffe (19,20).The sequence of plasmid pColE1 is numbered beginning at the first T in the EcoRI site (21), and the sequence of the replicated form of ΦX174 is numbered from the last G in the PstI site (22).

High Resolution Mapping Procedure

A solution of rhodium complex (10 μM) and plasmid DNA (83 μM nucleotides) in 5 mM Tris HCl, 50 mM NaCl, pH 7 is irradiated for 3.5 min at 332 nm. This irradiation converts approximately 70% form I DNA into cleaved species. Following irradiation, the DNA is ethanol precipitated twice so as to remove the rhodium complex. DNA is resuspended in Bgl 1 reaction buffer and digested with 15 units Bgl 1 for 1.5 h at 37 C. After phenol extraction and ethanol precipitation, the linearized DNA is resuspended in an appropriate reaction buffer for ^{32}P-labelling. For labelling at the 5'-end, bacterial alkaline phosphatase is first added to remove the 5'-phosphate, and T4 polynucleotide kinase is then added as is γ-^{32}P-ATP (specific activity 6000 Ci/mMol). Since Bgl 1 produces 3'-protruding ends, for labelling of the 3'-end, T4 polymerase is added as is α-^{32}P-GTP (specific activity 800 Ci/mMol). After a second digest with Alu 1 (10 units, 1.5 h at 37 C) the desired fragment is then isolated on a 5% polyacrylamide gel. The purified 448 bp fragment labeled at the 5'-end corresponds to the sequence from 3036 to 3484 with the label at the 3489 position. The 448 bp fragment labeled at the 3'-end spans positions 3036-3484 bp with the label at the 3484 position. The purified fragments are denatured and resolved on a 6% polyacrylamide denaturing gel. Untreated fragment is sequenced by the method of Maxam and Gilbert and coelectrophoresed on the same gel to determine the precise sites of cleavage by the metal complex (23). Gels are exposed to Kodak XAR-5 films at -60C for 1-7 days.

S1 Nuclease Probe of Metal Binding Sites

Plasmid pBR322 (100 μM nucleotide) in 50mM Tris acetate buffer containing 18mM of NaCl, pH7, is incubated for one minute, either in buffer alone or in buffer containing 10 μM rhodium complex. Thereafter, $ZnSO_4$ to a concentration of 1mM and 10 units S1 nuclease are added and the mixture is incubated for 5 min at 37 C. The reaction is quenched with the addition of ethanol. Samples are then resuspended in enzyme reaction buffer, combined with 8 units restriction enzyme for digestion, and electrophoresed as described above.

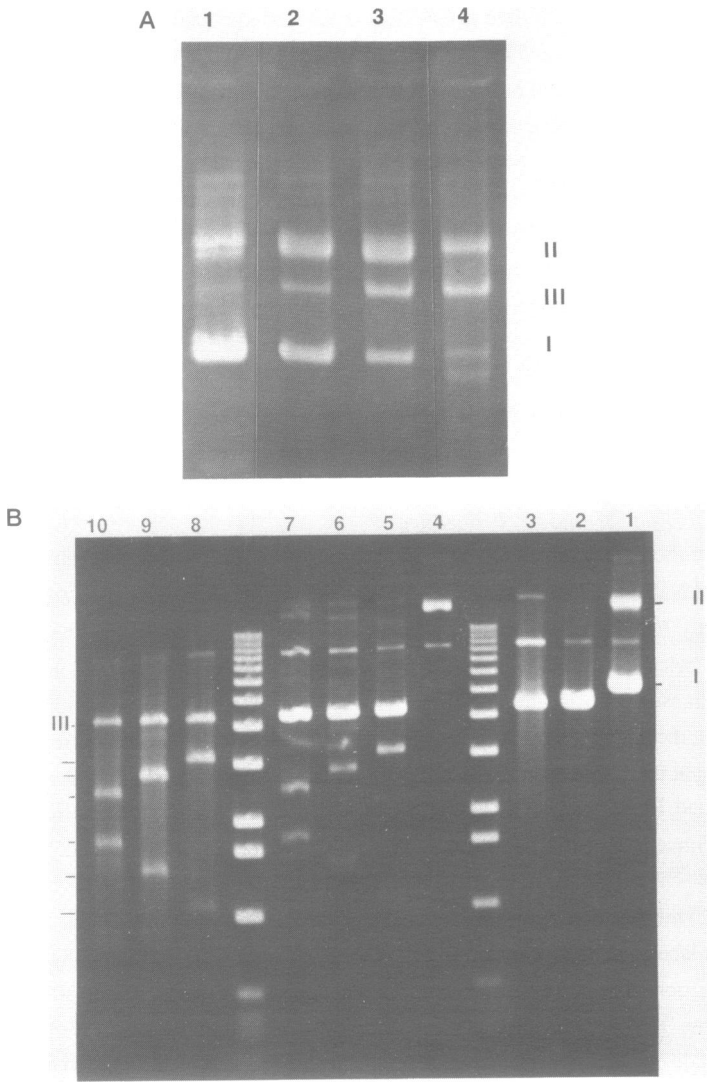

Figure 1: A. Agarose (1%) gel illustrating DNA photocleavage by $Rh(DIP)_3^{3+}$ with the production of form II and form III DNA: Lane 1, 100 μM pBR322 (nucleotides) in the absence of rhodium complex photolysed for 90 seconds; lanes 2-4, with 10 μM $Rh(DIP)_3^{3+}$ photolysed for 30, 60, and 150 seconds, respectively. B.Agarose (1%) gel indicating the photoinduced fragmentation of pBR322 by $Rh(DIP)_3^{3+}$ and coarse mapping technique (see "Experimental"). Lanes 1-3: pBR322 in the absence of rhodium complex and photolysed for 20 seconds before linearization; after linearization with Hind III; and after linearization and S1 nuclease digestion. Lanes 4-7: DNA photolysed in the presence of $Rh(DIP)_3^{3+}$ before linearization (4) and showing double-stranded fragmentation (5-7) after linearization with Hind III, Bam H1, and Ava I, respectively. Lanes 8-10 , same as 5-7, followed by S1 nuclease digestion. Other lanes are MW markers containing the following size fragments in bp: 1018, 1636, 2036, 3054, 4072, and 5090, respectively.

RESULTS AND DISCUSSION

Photo-induced DNA cleavage by the metal complex

Upon irradiation, $Rh(DIP)_3^{3+}$ induces both single and double stranded DNA cleavage. Figure 1 illustrates photocleavage of pBR322 DNA by $Rh(DIP)_3^{3+}$ and the coarse level mapping of specific sites of reaction. As may be apparent in Figure 1A, irradiation of pBR322 (100 μM nucleotides) in the presence of 10 μM rhodium complex, with 315-360 nm light, yields both nicked form II and linear form III DNA, and in proportions which indicates non-random double-stranded cleavage. After 1 minute irradiation, for example, 21% form II and 25% form III DNA are produced No cleavage is observed by the complex in the absence of light.

Sites of metal-promoted cleavage

A low resolution mapping procedure (5) is employed on the full plasmid to determine whether the single and double-stranded cleavage events induced by the metal complex occur at specific sites on the plasmid and if so, their locations. Following irradiation in the presence of $Rh(DIP)_3^{3+}$, the DNA is linearized with a single-site restriction enzyme. If the double-stranded cleavage induced by the metal complex is site-specific (at this resolution), a pair of distinct lower molecular weight fragments will be obtained in addition to the full linear species after electrophoresis. The position of specific double-stranded cleavage can then be determined from the lengths of the fragments obtained (to determine the site uniquely, two different restriction enzymes must be employed). Sites of specific single-stranded cleavage are determined similarly after further digestion of the photocleaved and linearized DNA with S1 nuclease, which cleaves opposite the rhodium-induced nick, thereby converting nicked linear DNA to doubly cleaved fragments.

A typical mapping gel, obtained after photocleavage of supercoiled pBR322 in the presence of racemic $Rh(DIP)_3^{3+}$ is given in Figure 1B. Photolysis of pBR322 DNA with $Rh(DIP)_3^{3+}$, followed by enzyme digestion with three different single-site restriction enzymes each leads to the production of two distinct bands, indicating that linearization by $Rh(DIP)_3^{3+}$ is specific to a site. With subsequent digestion with S1 nuclease, these fragment bands intensify and additional fragment bands become apparent. No specific fragments are produced after photolysis and digestion in the absence of rhodium. Photolysis experiments performed with DIP ligand itself or with $RhCl_3 \cdot 3H_2O$ reveal 12% and 0% form II DNA, respectively, relative to suitable light controls, too little cleavage to detect any specific bands using this mapping technique.

The sites of specific double-stranded cleavage on pBR322 DNA by $Rh(DIP)_3^{3+}$, determined by densitometric analysis of at least six experiments with four different restriction enzymes (Nde1, Hind III, BamH1 and Ava 1) are given in Table 1. The major cleavage site at 3250 bp results primarily from double-stranded cleavage and accounts for 90% of all specific cleavage by $Rh(DIP)_3^{3+}$ on pBR322. Two additional sites, at 4220 bp and 2300 bp, account for the remaining 10% cleavage; these are revealed more easily after further digestion with S1 nuclease. Experiments conducted using enantiomerically enriched (greater than 90%) metal complexes showed similar specificities as compared to the racemic mixture.

Table 1: Sites of Double Stranded Cleavage by $Rh(DIP)_3^{3+}$

DNA	Location of $Rh(DIP)_3^{3+}$ Cleavage sites[a] (Kbp)	Location(s) of Palindromic Repeat(s) (Kbp)	Size of Stem (bp)	Size of Loop (bp)	Reference
pBR322	3.25 +/-0.07[b]	3.0650 3.2205 3.1230	11 10 9	3 6 5	(19,20)
pColE1	0.09 +/-0.20	0 .1005	13	5	(21)
ΦX174 (rf II)	2.25 +/-0.11 4.14 +/-0.11 3.07 +/-0.10	2.3300 3.9650 3.0085	13[c] 9 8	2 3 8	(22)

[a] Averages were calculated from at least 6 experiments with at least 2 restriction enzymes, where the error given is 1σ.

[b] Sites of single stranded cleavage were also determined by S1 nuclease assays (see experimental) and were found at 4.22 +/-0.08 and 2.30 +/-0.06 kbp.

[c] The palindromic sequence contains a single internal incorrect purine-pyrimidine pairing.

At native superhelical densities in the presence of 50 mM NaCl, three cruciform sites were detected on pBR322 using an S1 nuclease assay (8). These correspond to the major (11bps), minor (10 bps), and subminor cruciform sites (9 bps), with inverted repeat sequences centered at 3065, 3221, and 3123 bp, respectively. The primary site for double stranded cleavage by $Rh(DIP)_3^{3+}$ corresponds to the region containing these three cruciforms and in particular is centered on the site of the minor cruciform on pBR322. If cleavage were, however, also obtained at the major cruciform site, it could not be distinguished in experiments at this resolution. The remaining sites for single-stranded cleavage by $Rh(DIP)_3^{3+}$ must correspond to distinctive conformations other than cruciforms and in fact parallel results obtained earlier for the locations of conformationally distinct sites using Λ–$Co(DIP)_3^{3+}$ as a probe (5).

Effects of salt and superhelicity

So as to characterize and better distinguish the site of linearization by $Rh(DIP)_3^{3+}$ from the remaining sites cleaved, cleavage under different conditions of salt and superhelicity were examined. Photolysis in buffer containing 18 mM NaCl, with subsequent NdeI digestion, produces 4 fragment bands centered at 3.5, 2.5, 1.9, and 1.0 Kbp, as shown in trace A of Fig. 2. These fragment lengths map to the cleavage sites for $Rh(DIP)_3^{3+}$ at 3.2 and 4.2 Kbp on pBR322. Under the same experimental constraints, except in the presence of 150 mM NaCl as shown in trace B, the same fragment bands are apparent, but with diminished intensities. Longer (approximately 3x) periods of photolysis are required to achieve similar amounts of form II and form III DNA in the presence of the higher concentration of NaCl. Consistent with earlier results using other metal complexes (24), binding of the rhodium complex to the DNA decreases with increased salt. The comparison of densitometric scans in traces A and B of Fig. 2, however, indicate further a change in relative intensity of fragments with increasing salt. With increasing salt, bands centered at 2.5 and 1.9 Kbp increase in intensity relative to those at 3.5 and 1.0 Kbp.

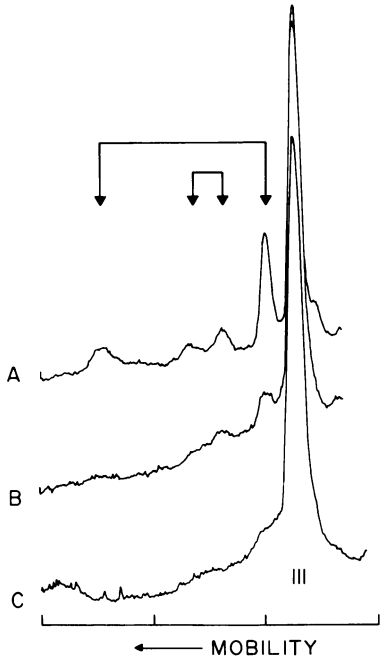

Figure 2: Densitometric scans after fragmentation of pBR322 by $Rh(DIP)_3^{3+}$ in differing salt concentrations and differing superhelicity: Trace A: supercoiled pBR322 photolysed with $Rh(DIP)_3^{3+}$ for 1 minute in running buffer containing 50 mM tris pH 7.0, 18 mM NaCl, and 20 mM NaOAc). Trace B: same as A except photolysed for 3 minutes in running buffer containing 150 mM NaCl. Trace C: linearized pBR322 photolysed with $Rh(DIP)_3^{3+}$ for 1 minute in running buffer. Nde I was used for linearization in all samples. Fragment pairs are indicated.

This result reflects the differing dependence of the two conformations marked by the metal complex on ionic strength; the distinct conformation centered at 3.2 Kbp, the cruciform site, diminishes more rapidly with increased ionic strength. Cleavage experiments were conducted also in the presence of increasing concentrations of Mg^{2+}, which is known to affect cruciform extrusion and geometry (11). Specific double-stranded cleavage by $Rh(DIP)_3^{3+}$ at the cruciform site is observed in the presence of 1 mM Mg^{2+}. With 10 mM Mg^{2+}, specific sites of cleavage are no longer apparent.

The conformations at both sites do, however, based upon specific cleavage by the metal complexes, require supercoiling of the plasmid. Initial linearization of pBR322 by Nde I, followed by irradiation with $Rh(DIP)_3^{3+}$ and S1 nuclease digestion, as shown in trace C of Fig. 2, reveals no detectable specific fragmentation. Similar experiments performed on the linear template using other restriction enzymes for linearization corroborate this finding. Consistent with the requirements of cruciform formation, then, DNA supercoiling (native superhelical density) is needed for recognition of the cruciform site by the metal complex.

Targeting of cruciforms by $Rh(DIP)_3^{3+}$ on other DNAs

So as to explore whether cleavage of cruciforms by the rhodium complexes is general or particular only to the cruciform on pBR322, we examined also other plasmids containing extruded cruciform structures at native superhelical density. As was found for cleavage by the rhodium complex on pBR322, cleavage of the replicative form of ϕX174 DNA and pColE1 DNA yields also a higher extent of double stranded cleavage than would be expected given two nearby random single-stranded cleavage events. Table 1 summarizes also coarse mapping results for double-stranded cleavage by the rhodium complex on ϕX174 DNA and pColE1 DNA. The replicative form of ϕX174 DNA was shown earlier by computer searches to contain two perfect palindromic sequences (7), and one imperfect palindromic sequence (13). From similar computer searches pColE1 DNAwas found to contain one palindromic sequence (13). Sites of double-stranded cleavage by the rhodium complex map to the regions containing these sequences. Many cruciform sites lie in AT-rich sequences of DNA. The rhodium complex at least appears to recognize a cruciform-containing AT-rich segment rather than simply the AT-rich domain, since both ϕX174 and pBR322 contain several AT-rich regions (>70% AT) that lack palindromic sequences and are not linearized by $Rh(DIP)_3^{3+}$. Specific sites of single stranded cleavage by the rhodium complex on these plasmids are also revealed after subsequent digestion with S1 nuclease, but their locations have not been determined.

Figure 3 shows the results of the specific fragmentation by $Rh(DIP)_3^{3+}$ on these closed circular DNAs after linearization with a single site restriction enzyme and provides also a comparison in the specificity of cruciform cleavage between the rhodium complex and S1 nuclease. As can be seen in Figure 3, linearization of ϕX174 with Pst I, after cleavage by the rhodium complex, yields four distinct lower molecular weight fragments, consistent with the double-stranded targeting by the rhodium complex of two cruciform sites on the DNA. Similarly, after photocleavage with $Rh(DIP)_3^{3+}$, linearization of pColE1 DNA using Cla I yields two distinct fragments, consistent with the presence of one cruciform on the plasmid at native superhelical densities. The comparison in cleavage using $Rh(DIP)_3^{3+}$ versus S1 nuclease is, in addition, quite clear for pColE1. Bands are apparent at similar mobilities using both the enzymatic and inorganic probes, yet cleavage with S1 nuclease contains also a background level of non-specific degradation and the band pattern is more diffuse than that obtained with the rhodium complex. For ϕX174, the S1 nuclease degradation pattern differs from that of $Rh(DIP)_3^{3+}$ and points to a variety of hypersensitive sites, more than may be accounted for based upon cruciform recognition. In comparison to S1 nuclease reactivity, then, $Rh(DIP)_3^{3+}$ may offer a more specific and sensitive route to detect cruciform structures.

Using S1 nuclease to probe the site of metal binding

So as to investigate the possibility that $Rh(DIP)_3^{3+}$ may promote cruciform formation and so as to compare S1 nuclease cleavage at cruciform sites with rhodium photocleavage, we examined sites of rhodium binding in the presence of S1 nuclease using the nuclease rather than metal

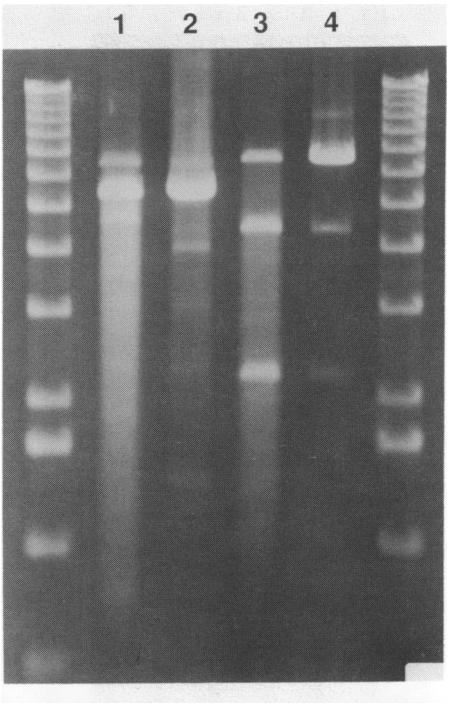

Figure 3: Agarose (1%) gel comparing the fragmentation of φX174 and pColE1 by $Rh(DIP)_3^{3+}$ and S1 nuclease. Lanes 1 and 2 show φX174 (rf II) after cleavage by S1 nuclease or $Rh(DIP)_3^{3+}$ with photolysis (2 min), followed by linearization with Pst I. In addition to the strong linear band, four lower molecular fragments are evident upon rhodium photocleavage, corresponding to recognition of the two cruciform sites. Lanes 3 and 4 show pColE1 after cleavage by S1 nuclease or $Rh(DIP)_3^{3+}$ with photolysis (2 min), followed by linearization with Cla I. Here a similar pattern is evident upon treatment with the nuclease or rhodium complex.

photoactivation to mark these sites. Fig. 4 shows, after linearization with BamHI, fragmentation of pBR322 DNA by $Rh(DIP)_3^{3+}$ with light, fragmentation with S1 nuclease in the presence of rhodium (no light), and fragmentation by S1 nuclease in the absence of the added metal complex. It should be noted that in these experiments S1 nuclease treatment precedes linearization, maintaining the altered conformations, rather than following the linearization step as for the coarse mapping experiments of singly cleaved regions described earlier. In the absence of rhodium, S1 nuclease marks, though not sharply, the major and minor sites of cruciform formation. The S1 nuclease map in the presence of rhodium is distinctly different, however, and instead parallels fragmentation seen upon photocleavage by $Rh(DIP)_3^{3+}$. With $Rh(DIP)_3^{3+}$ and S1 nuclease, two fragments are distinctly evident. These fragments correspond to those produced in the photocleavage reaction of pBR322 DNA and $Rh(DIP)_3^{3+}$ as shown in lane 2 of Fig. 4. This enhanced cleavage at the rhodium binding sites may be an indication that rhodium binding does

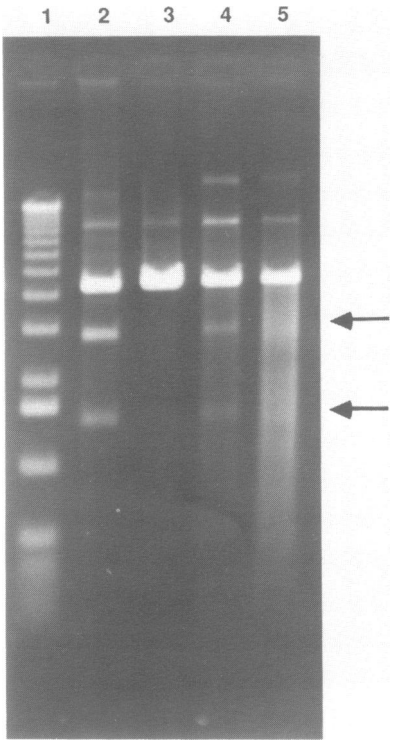

Figure 4: Agarose (1%) gel marking the binding sites for $Rh(DIP)_3^{3+}$ on pBR322 using S1 nuclease. Lanes 2-3: closed circular pBR322 treated with light in the presence or absence of racemic $Rh(DIP)_3^{3+}$, followed by linearization with Bam H1. Lanes 4-5: pBR322 treated with S1 nuclease in the presence or absence of racemic $Rh(DIP)_3^{3+}$ followed by linearization with Bam H1.

promote extrusion of cruciforms. Densitometric analysis of this and three other experiments, however, reveal S1 nuclease cleavage sites in the presence of $Rh(DIP)_3^{3+}$, in order of decreasing activity, to be at 3230 ± 80, 2300 ± 100, 4300 ± 60, and 1500 ± 100 bp respectively. These sites actually include all the sites of cleavage by $Rh(DIP)_3^{3+}$, both the cruciform and non-cruciform structures. Therefore another explanation for the enhanced pattern of cleavage by S1 nuclease shown in Figure 4 may be that binding of the rhodium to any DNA site, irrespective of its initial structure, sufficiently perturbs the local DNA structure (for example if the metal complex intercalates) so as to enhance the sensitivity of sites to reaction with S1 nuclease. At a cruciform site both reaction by S1 nuclease in the loop region and at the rhodium binding site then become available. Cleavage by S1 nuclease in the presence of $RhCl_3$ was also tested to determine if the rhodium trication alters S1 nuclease specificity. This control showed fragmentation identical to that by S1 nuclease in the absence of any rhodium complex.

Binding and cleavage on linear versus supercoiled substrates was also compared by S1 nuclease treatment of the substrates in the presence and absence of $Rh(DIP)_3^{3+}$. S1 nuclease cleavage of linear pBR322 DNA after incubation of the linear polymer with $Rh(DIP)^{3+}$ revealed no specific pattern of fragmentation. This result indicates that $Rh(DIP)_3^{3+}$ neither binds to nor promotes distinct conformations on the linear template. If some stabilization of cruciform structure occurs upon rhodium binding, it is then insufficient to drive such transitions in the absence of supercoiling.

High resolution map of $Rh(DIP)_3^{3+}$ cleavage near a cruciform on pBR322

Since it is clear from low resolution experiments that $Rh(DIP)_3^{3+}$ linearizes DNA in the vicinity of cruciforms, we examined at higher resolution the site(s) of cleavage by $Rh(DIP)_3^{3+}$ near the cruciform centered at 3250 bp on pBR322. After photocleavage of the supercoiled plasmid in the presence or absence of the rhodium complex, ^{32}P-end-labeled fragments (3000-3400 region) were isolated and examined. Figures 5A and 5B show autoradiographs of sequencing gels containing the 3'- and 5'- end labeled fragments containing the cruciform region cleaved by $Rh(DIP)_3^{3+}$ and Fig. 6 summarizes the results. At this resolution, it is clear that $Rh(DIP)_3^{3+}$ does indeed cleave primarily at one strong site on each strand neighboring the cruciform.

Several points are noteworthy. First, and perhaps foremost, as is evident in Fig. 5, on the 448 base pair fragment, one primary site at position 3238 on the 3'-labeled strand and one site at position 3250 on the 5'- strand are cleaved quite specifically by the metal complex. Cleavage at these sites on the two strands of the supercoiled plasmid would account for the linearization of the DNA. Furthermore, as might be expected for photo-oxidation with the rhodium complex (6), cleavage on each strand occurs at a single interbase pair position, rather than over several bases as would be expected if cleavage were mediated by a diffusing species such as hydroxyl radical. Figure 6 shows the location of these cleavage points relative to that of the extruded cruciform. The strong cleavage sites are actually apparent not at the cruciform loop but are instead located on one side of the base of the cruciform. The specificity associated with targeting this distinctive site is remarkable. The intensity of cleavage by the metal complex at this position is more than ten times greater than that found with the complex at any other position evident on these gels. It is interesting also that the pattern is asymmetric with respect to the cruciform. No cleavage is evident on the other side of the stem.

This site-specific cleavage is, however, governed by the formation of the cruciform. An additional strong cleavage site (3080 +/- 5 bp) is observed on this fragment (5'-end-labeled strand), when electrophoresed for longer periods, at the position consistent with that of the major cruciform site on pBR322 (the lack of availability of convenient restriction sites made high resolution examination of this site impractical). Furthermore, recognition and reaction by the complex requires supercoiling. As is apparent in comparing lanes 3 with 5-7 of Figure 5A, if the DNA is linearized first and then photolyzed in the presence of the rhodium complex, no specific cleavage is observed. Therefore, it is not simply the sequence of bases that is determining the

reaction with the complex. While primary cleavage is not directly in the cruciform but is instead to its side, this distinct structure, the topology associated with the site rather than simply the sequence, must be important to the recognition.

The fact that the complex cleaves on only the AT-rich side flanking the cruciform, however, may actually reflect some sequence selectivity of the complex or some structural asymmetry in the site that is a function of the AT-rich site. The topology associated with this side of the cruciform may be more accessible to the complex; AT-sites are thought to "breathe" under

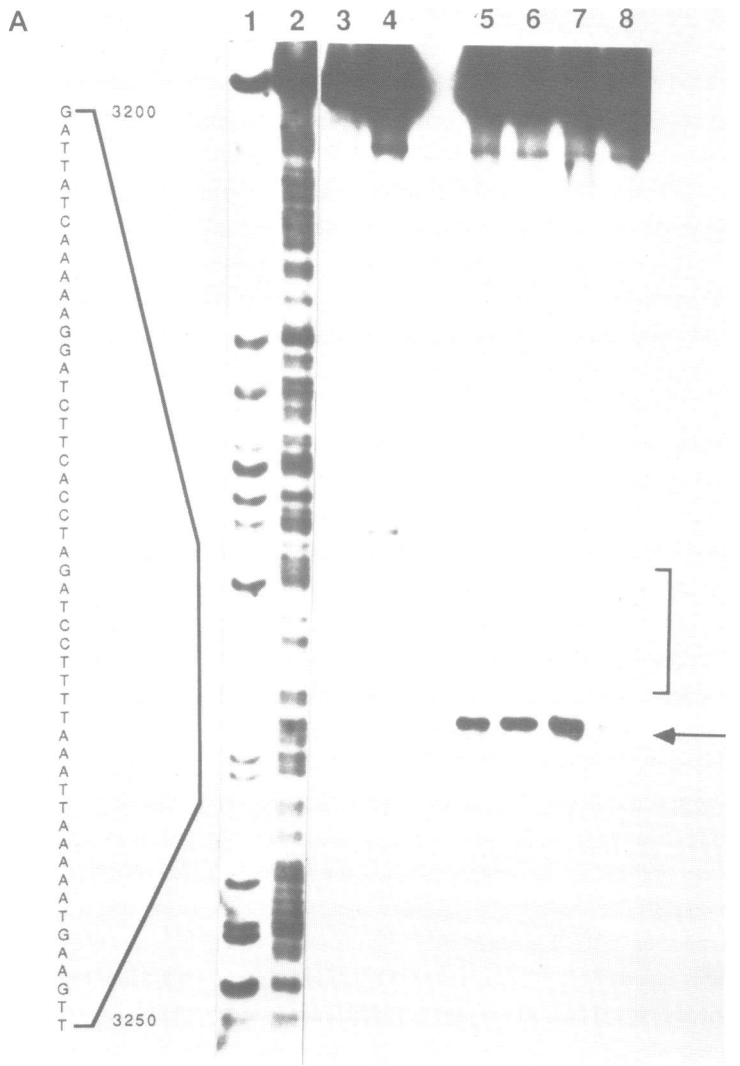

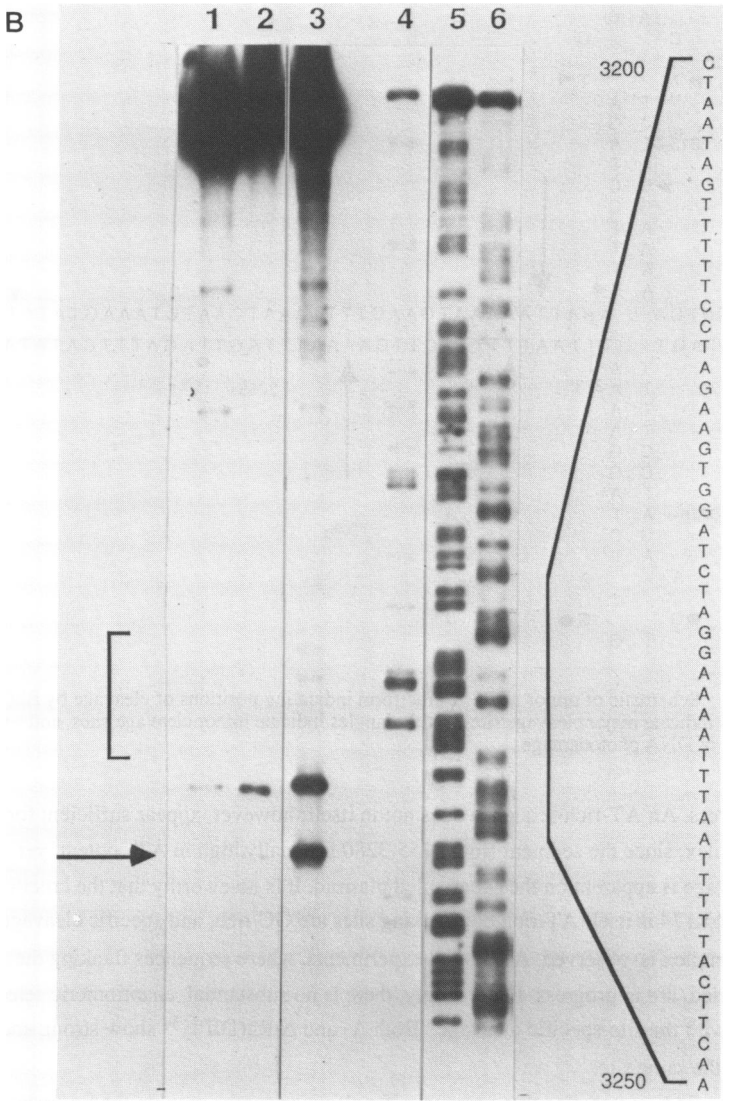

Figure 5: High resolution map of 3000-3500 bp region of pBR322 illustrating specific cleavage by $Rh(DIP)_3^{3+}$. Autoradiographs of denaturing polyacrylamide gels of 3'-labelled fragment (3036-3484*) in (A) and 5'-labelled fragment (3036-3484*) in (B), showing sites of cleavage on each strand. (A) Lanes 1-2, Maxam Gilbert G and G + A sequencing reactions; lanes 3-4, linearized fragment photolysed with and without racemic $Rh(DIP)_3^{3+}$; lanes 5-7, fragment isolated after closed circular pBR322 was photolysed in the presence of either racemic, Δ, or Λ-$Rh(DIP)_3^{3+}$, respectively; and lane 8, same conditions as in 5-7 excluding metal complex. (B) Lane 1, control DNA fragment isolated from pBR322; lanes 2-3, same as in 1 treated with light in the absence and presence of racemic $Rh(DIP)_3^{3+}$; lanes 4-6, Maxam Gilbert G, G + A and T+C sequencing reactions, respectively. The arrows delineate the positions of primary photocleavage by $Rh(DIP)_3^{3+}$. The palindromic sequence near the $Rh(DIP)_3^{3+}$ cleavage site in this fragment is indicated by the small brackets.

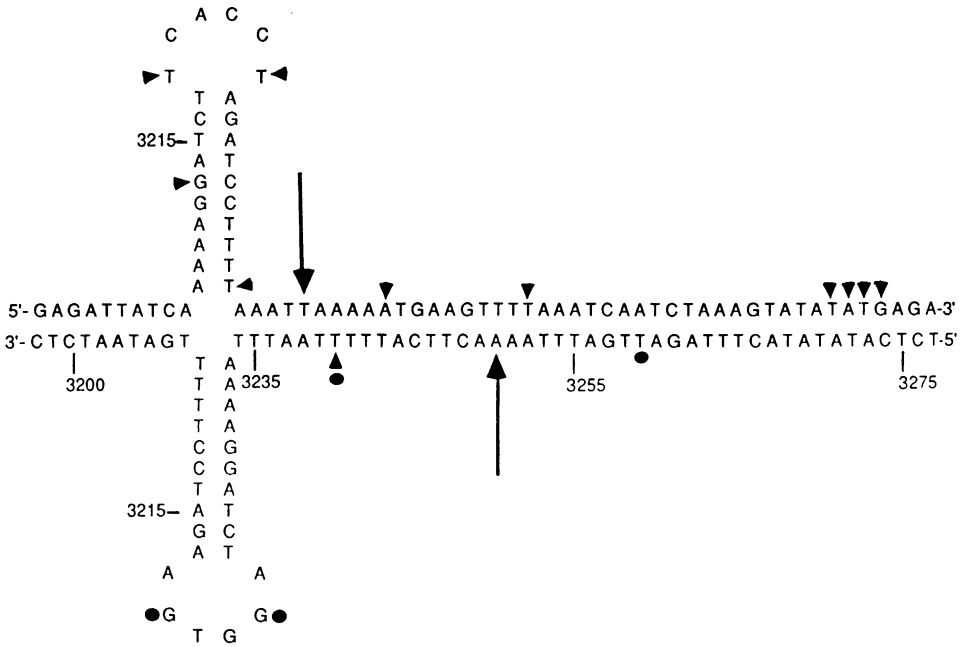

Figure 6: Schematic of minor pBR322 cruciform indicating positions of cleavage by $Rh(DIP)_3^{3+}$. Large arrows indicate major cleavage sites, solid triangles indicate minor cleavage sites, and solid circles indicate sites of DNA photodamage.

torsional stress. An AT-rich sequence does not in itself, however, appear sufficient for recognition by the complex, since the segment from 3255-3280 is equally high in AT content, yet no similarly strong cleavage is apparent on the supercoiled plasmid. It is noteworthy that the cruciform centered at 2330 on ϕX174 is itself AT-rich but flanking sites are GC-rich, and specific cleavage by the rhodium complex is observed. Additional experiments, where sequences flanking the cruciform sites are varied, are in progress. Interestingly, there is no substantial enantiomeric selectivity associated with the site-specific cleavage. Both Λ- and Δ-$Rh(DIP)_3^{3+}$ show strong and specific cleavage at the same site.

It should be noted also that some specific cleavage can be seen on the fragment even without the rhodium complex, and this damage, we attribute to the ultraviolet photolysis. Figure 5B shows most clearly the specific photodamage at position 3240 on the 5'-end-labeled fragment. This site corresponds to a tract of 5 thymines in a row. Cleavage at this site is found to be greater in the presence of the rhodium complex. Figure 6 indicates additional sites of weaker damage on each fragment. These appear to be associated primarily with thymine-rich sequences and presumably result from the formation of thymine dimers. Some damage is evident also in the loop region of the cruciform (also on the 5'-end-labeled fragment) and this may reflect reaction with single-strand nuclease.

Additional cleavage, though substantially weaker, is induced at other sites by the metal complex upon photolysis. Some cleavage is evident, for example, both in the loop and stem of the 3'-end-labeled fragment, but no similar cleavage is found on the other strand. This metal-promoted damage may be indicative either of metal binding to the cruciform stem itself or, more likely, the bending over (or knotting) of the cruciform stem onto the main helix. This structural change would be consistent with the asymmetric cleavage by the rhodium complex only on one side of the cruciform. Weak cleavage is evident also in the nine-base pair alternating purine-pyrimidine stretch (3270 bp). This site of cleavage may reflect partial conversion of the region into a left-handed conformation; Λ-$Rh(DIP)_3^{3+}$, essentially identical in structure to its cobalt analogue, could, like the cobalt complex, be expected to recognize and react at left-handed sites.

Recognition of the Cruciform Structure

What does the specific cleavage by the rhodium complex indicate about the structure of the cruciform site? There have been several models proposed for cruciform structures, including tetragonal and tetrahedrally disposed helices as well as lower order structures where helices may stack on each other so as to form two parallel helical domains (7, 8, 25). While our data cannot distinguish between these models, the results are certainly consistent with an asymmetry in the cruciform site. The rhodium complex reveals this asymmetry by cleaving only to one side of the cruciform stem. Perhaps the hydrophobic metal complex is recognizing a small pocket produced by an association of the two helical regions. If, for example, the helical segment produced by intrastrand hydrogen bonding of the 5'-strand were to fold back onto the strand in the 3'-direction, an enclosed space between helices would result. The AT-rich sequence, furthermore, may be particularly important here, either as a recognition element for the complex or in determining the different folding and topological characteristics of the site. It is noteworthy, in the context of a looped-back model, that although the predominant cleavage site for the rhodium complex is on the interstrand hydrogen-bonded region upstream of the cruciform, some damage is evident by the rhodium complex on the 5'-strand cruciform stem itself. If the rhodium complex were tightly bound to the main helix but enclosed by the folded cruciform, some reaction along the helical stem, presumably through activation of an ancillary ligand on the complex, might result. Such folding or association of helical segments has precedence in, for example, the structure of tRNA. Hoogsteen pairing, which is possible between homopurine and homopyrimidine stretches on each helix, might further stabilize a closed structure. Models for Holliday junctions suggest also a reduction in symmetry in junction sites through the formation of interstacked side-by-side helical segments (25); no obvious explanation for our pattern of cleavage could be derived from such a model, however. It is noteworthy, in addition, in considering the asymmetry associated with cruciform sites, that T4 endonuclease VII cleaves only the 5'-side of the inverted repeat (each strand) of this cruciform (15). Furthermore, the peptide fragment of Hin recombinase linked to $Fe(EDTA)^{2-}$ recognizes also this region containing the minor cruciform on a linearized pBR322 fragment (3202 bp) , even though the sequence homology with the primary binding site for the recombinase is low (26).

What features of the structure are important to recognition and reaction by the rhodium complex? $Rh(DIP)_3^{3+}$ resembles very closely, from a structural and electrostatic standpoint, its analogue $Co(DIP)_3^{3+}$. Bond distances for Rh-N are typically 2.04 A (27) and for Co(III)-N are 1.95 A (28), and thus a difference in size of 0.1 A over a complex having a diameter of approximately 25 A is unlikely to affect recognition on the helix. Therefore it is not surprising that sites cleaved, either in a double-stranded or single-stranded fashion, on pBR322 by racemic-$Rh(DIP)_3^{3+}$ include those cleaved by Λ-$Co(DIP)_3^{3+}$. The surprising difference between the complexes, however, is with regard to the extent of double-stranded cleavage seen only with the rhodium complex (either enantiomer) at the cruciform site. This difference must then result not from binding characteristics but from a difference in photochemistry. Like the cobalt analogue, rhodium(III) polypyridyl complexes are efficient photo-oxidants (actually more efficient than the analogous cobalt species) (6). The complexes differ, however, in that once reduced, ligand lability for the cobalt(II) product is high, permitting ligand dissociation, whereas for the rhodium species, ligand lability would still be quite slow, possibly, then, facilitating instead reoxidation and a second round of photoreaction.This difference in lability could account for the perponderance of double-stranded cleavage events by $Rh(DIP)_3^{3+}$; at the cruciform site, the residence time of the complex on the site may be sufficiently long to facilitate the double reaction. An alternate proposal for the double-stranded cleavage would require the association of two complexes at the bound site. But such an association would be available both to the cobalt as well as rhodium analogues; cleavage of pBR322 with rac-$Co(DIP)_3^{3+}$ shows no similar non-random double-stranded cleavage. The notion of the rhodium complex showing enhanced cleavage at a site bound with a particularly long residence time would also be consistent with the idea of recognition of an interhelical pocket at the cruciform. The rhodium complex shares with its cobalt analogue other features as well in reactions at DNA sites. Photoinduced cleavage for both species is specific to a single interbase position and indicates no diffusing species. Furthermore, cleavage on the two strands is, both for the rhodium and cobalt complex (4), asymmetric to the 5' side. Thus the pattern of cleavage might be consistent with access from the major groove. Disturbing, however, in this case is the fact that the cleavage sites are separated by 12 base pairs. The complex itself spans at least eight base pairs, and an eight base pair separation in cleavage on the two strands has been observed for the cobalt analogue (4). Still, despite the large size of the complex, the pattern of cleavage seen here would require quite a shallow pitch of the helix or, perhaps more likely, an alternately perturbed structure in this region.

Most important regarding cleavage by the rhodium complex at the cruciform site is its remarkable level of specificity. This specificity is based upon the targeting by the complex of a distinctive structure, that of a cruciform, rather than of a unique sequence. Cruciforms of different sequences are recognized by $Rh(DIP)_3^{3+}$, and for a given palindromic sequence, if it is not extruded into a cruciform, as for the case of the linearized plasmid, no cleavage by the metal

complex is observed. *The specificity for the double-stranded reaction by the complex at a given site is based, then, not simply on sequence selectivity but instead upon shape selectivity.* $Rh(DIP)_3^{3+}$ contains neither hydrogen bonding donors nor acceptors. It possesses, instead, a well-defined hydrophobic structure held together by the central and coordinatively saturated metal ion. The specific double-stranded cleavage of cruciform sites by $Rh(DIP)_3^{3+}$ reported here suggests that the rhodium complex may be generally useful as a reagent to probe cruciform sites. Moreover the remarkable site-specificity of these reactions underscores once again a useful approach to the targeting of specific sites on a DNA strand through the development of shape-selective molecules.

ACKNOWLEDGEMENTS

We are grateful to the National Institutes of Health (GM33309), the National Foundation for Cancer Research, and the Swiss National Science Foundation (to R.T.) for their generous support of this research.

*To whom correspondence should be addressed

REFERENCES

1. Barton, J.K.(1986) *Science*, **233**, 727-734.
2. Mei, H.Y., Barton, J.K.(1988), *Proc. Natl, Acad, Sci., USA*, **85**, 1339-1343.
3. Mei, H.Y., Barton, J.K.(1986), *J. Am. Chem. Soc.* **108**, 7414-7416.
4. Meuller, B.C., Raphael, A.L., Barton, J.K.(1987), *Proc. Natl. Acad.Sci.USA* **84**, 1764-1768.
5. Barton, J.K., Raphael, A.L.(1985), *Proc. Natl. Acad. Sci. USA* **82**, 6460-6464.
6. Fleisher, M.B., Waterman, K.C., Turro, N.J., Barton, J.K. (1986), *Inorganic Chemistry* **25**, 3549-3551.
7. Platt, J.R. (1955) *Proc. Natl. Acad. Sci. USA* **41**, 181-183; Gierer, A. (1966) *Nature* **212**, 1480-1481.
8. Lilley, D.M.J., Sullivan, K.M. and Murchie, A.I.(1987) Eckstein, F. and Lilley, D.M.J. (eds), *Nucleic Acids and Molecular Biology, Springer Verlag Heidelberg,Vol. I.*,pp. 126-137.
9. Lilley, D.M.J., Markham, A.F. (1983) *EMBO J* . **2**, 527-533.
10. Lilley, D.M.J.(1985) *Nucl. Acids Res.* **3**, 1443-1465.
11. Sullivan, K.M. and Lilley, D.M.J.(1987), *J. Mol. Biol.* **193**, 397-404.
12. Lilley, D.M.J., (1983) *Nucl. Acids Res.* **11**, 3097-3112; Lilley, D.M.J. and Palecek, E. (1984) *EMBO J.* **3**, 1187-1192.
13. Lilley, D.M.J., (1980), *Proc. Natl.. Acad. Sci. USA* **77**, 6468-6472.
14. Sinden, Richard R. and Pettijohn, David E. (1984) *J. Biol. Chem.* **259**, 6593-6600.
15. Lilley, D.M.J., Kemper, B. (1984) *Cell* **36**, 413-422.
16. Gillard, R.D. and Heaton, B.T. (1972) *Coordination Chemistry Reviews* **8**, 150- 157.
17. Gillard, R.D. and Dollimore, L.S.(1973) *JCS Dalton Transactions*, 939-9.
18. Barton, J.K. and Nowick, J.S. (1984), *JCS Chemical Communications* , 1650-2.
19. Sutcliffe, J.G.(1979) *Cold Spring Harbor , Symp. Quant. Biol.* **73**, 77-90.
20. Sutcliffe, J.G.(1978) *Proc. Natl. Acad. Sci. USA* **75**, 3737-3741.
21. Chan, P.T., Ohmori, H. Tomizawa, J. and Lebowitz, J. (1985) *J. Biol. Chem.* **260** 8925-8935.

22. Sanger, F., Coulson, A.R., Friedmann, T., Air, G.M., Barrell, B.G., Brown, N.L., Fiddes, J.C., Hutchison, C.A., III., Slocombe, P.M., & Smith, M. (1978) *J. Mol. Biol.* **125**, 225-246.
23. Maxam, A.M. and Gilbert, W.(1980) *Methods Enzymol.*, 499-560.
24. Raphael, A. L. (1987) Ph.D. thesis, Columbia University; Barton, J.K., Goldberg, J.M., Kumar, C.V., and Turro, N.J. (1986) *J. Am. Chem. Soc.* **108**, 2081-2088.
25. Sigal, N. and Alberts, B. (1972) *J. Mol. Biol.* **71**, 789-791.
26. Sluka, J.P., Horvath, S.J., Bruist, M.F., Simon, M.I., and Dervan, P.B. (1987) *Science* **238**, 1129-1132.
27. Ohba, S., Miyamae, H., Sato, S. and Saito, Y. (1979) *Acta Cryst.* **B35**, 1470-1472.
28. Yanagi, Ohashi, Y., Sasada, Y., Kaizu, Y., and Kobayashi, H. (1981) *Bull. Chem. Soc. Jpn.* **54**, 118-126.